

# 1 SARS-CoV-2 Infection of Salivary Glands Compromises Oral Antifungal Innate

## 2 Immunity and Predisposes to Oral Candidiasis

3 Areej A. Alfaifi<sup>1,2,3</sup>, Tristan W. Wang<sup>1</sup>, Paola Perez<sup>4</sup>, Ahmed S. Sultan<sup>1,5</sup>, Timothy F.  
4 Meiller<sup>1,5</sup>, Peter Rock<sup>6</sup>, David E. Kleiner<sup>7</sup>, Daniel S. Chertow<sup>8,9</sup>, Stephen M. Hewitt<sup>7</sup>,  
5 Billel Gasmi<sup>7</sup>, Sydney Stein<sup>8</sup>, Sabrina Ramelli<sup>8</sup>, Daniel Martin<sup>10</sup>, Blake M. Warner<sup>\*4</sup>,  
6 Mary Ann Jabra-Rizk<sup>\*1,11</sup>

7  
8     <sup>1</sup> Department of Oncology and Diagnostic Sciences, School of Dentistry, University of  
9     Maryland Baltimore, Maryland, United States of America

10 <sup>2</sup> Department of Restorative and Prosthetic Dental Sciences, College of Dentistry, King  
11 Saud bin Abdulaziz University for Health Sciences, Riyadh, Saudi Arabia

12 <sup>3</sup> King Abdullah International Medical Research Center (KAIMRC), Riyadh, Saudi Arabia  
13 <sup>4</sup> Salivary Disorders Unit, National Institute of Dental and Craniofacial Research, National  
14 Institutes of Health, Bethesda, Maryland, United States of America

15 <sup>5</sup> University of Maryland Greenebaum Cancer Center, University of Maryland Baltimore,  
16 Maryland, United States of America

17 <sup>6</sup> Department of Anesthesia, School of Medicine, University of Maryland Baltimore,  
18 Maryland, United States of America

19 <sup>7</sup> Laboratory of Pathology, Center for Cancer Research, National Cancer Institute,  
20 National Institutes of Health, Bethesda, Maryland, United States of America

<sup>8</sup> Critical Care Medicine Department, Clinical Center, National Institutes of Health

22 Bethesda, MD, USA

24 <sup>9</sup> Laboratory of Virology, National Institute of Allergy and Infectious Diseases, National  
25 Institutes of Health, Hamilton, MT, United States of America, USA

26 <sup>10</sup> Genomics and Computational Biology Core, National Institute of Dental and  
27 Craniofacial Research, National Institutes of Health, Bethesda, Maryland, United States  
28 of America

29 <sup>11</sup> Department of Microbiology and Immunology, School of Medicine, University of  
30 Maryland, Baltimore, Maryland, United States of America

31

32 **\* Corresponding authors**

33 Mary Ann Jabra-Rizk, PhD

34 E-mail address: [mrizk@umaryland.edu](mailto:mrizk@umaryland.edu)

35

36 Blake M. Warner, DDS, PhD, MPH

37 E-mail address: [blake.warner@nih.gov](mailto:blake.warner@nih.gov)

38

39 **Short title:** SARS-CoV-2 Infection of Salivary Glands Predisposes to Oral Candidiasis

40

41 **ABSTRACT**

42 Saliva contains antimicrobial peptides considered integral components of host innate  
43 immunity, and crucial for protection against colonizing microbial species. Most notable is  
44 histatin-5 which is exclusively produced in salivary glands with uniquely potent antifungal  
45 activity against the opportunistic pathogen *Candida albicans*. Recently, SARS-CoV-2 was  
46 shown to replicate in salivary gland acinar cells eliciting local immune cell activation. In

47 this study, we performed mechanistic and clinical studies to investigate the implications  
48 of SARS-CoV-2 infection on salivary histatin-5 production and *Candida* colonization. Bulk  
49 RNA-sequencing of parotid salivary glands from COVID-19 autopsies demonstrated  
50 statistically significant decreased expression of histatin genes. *In situ* hybridization,  
51 coupled with immunofluorescence for co-localization of SARS-CoV-2 spike and histatin  
52 in salivary gland cells, showed that histatin was absent or minimally present in acinar cells  
53 with replicating viruses. To investigate the clinical implications of these findings, salivary  
54 histatin-5 levels and oral *Candida* burden in saliva samples from three independent  
55 cohorts of mild and severe COVID-19 patients and matched healthy controls were  
56 evaluated. Results revealed significantly reduced histatin-5 in SARS-CoV-2 infected  
57 subjects, concomitant with enhanced prevalence of *C. albicans*. Analysis of prospectively  
58 recovered samples indicated that the decrease in histatin-5 is likely reversible in mild-  
59 moderate disease as concentrations tended to increase during the post-acute phase.  
60 Importantly, salivary cytokine profiling demonstrated correlations between activation of  
61 the Th17 inflammatory pathway, changes in histatin-5 concentrations, and subsequent  
62 clearance of *C. albicans* in a heavily colonized subject. The importance of salivary  
63 histatin-5 in controlling the proliferation of *C. albicans* was demonstrated using an *ex vivo*  
64 assay where *C. albicans* was able to proliferate in COVID-19 saliva with low histatin-5,  
65 but not with high histatin-5. Taken together, the findings from this study provide direct  
66 evidence implicating SARS-CoV-2 infection of salivary glands with compromised oral  
67 innate immunity, and potential predisposition to oral candidiasis.

68

69 **AUTHOR SUMMARY**

70 Saliva contains antimicrobial peptides part of host innate immunity crucial for protection  
71 against colonizing microbial species. Most notable is the antifungal peptide histatin-5  
72 produced in salivary glands cells. SARS-CoV-2 was shown to replicate in salivary gland  
73 cells causing tissue inflammation. In this study, we showed decreased expression of  
74 histatin genes in salivary glands from COVID-19 autopsies, and co-localization studies of  
75 SARS-CoV-2 spike and histatin revealed absence or minimal presence of histatin in  
76 acinar cells with replicating virus. To investigate the clinical implications of these findings,  
77 we conducted studies using saliva samples from subjects with mild to severe COVID-19,  
78 matched with healthy controls. Results revealed significantly reduced histatin-5 in SARS-  
79 CoV-2 infected subjects with enhanced prevalence of *C. albicans*. Prospective analysis  
80 indicated the decrease in histatin-5 is reversible in mild-moderate disease, and salivary  
81 cytokine profiling demonstrated activation of the Th17 inflammatory pathway. The  
82 importance of salivary histatin-5 in controlling the proliferation of *C. albicans* was  
83 demonstrated using an *ex vivo* assay where *C. albicans* was able to proliferate in saliva  
84 with low histatin-5, but not with high histatin-5. Collectively, the findings provide direct  
85 evidence implicating SARS-CoV-2 infection of salivary glands with compromised oral  
86 innate immunity and predisposition to oral candidiasis.

87

88 **INTRODUCTION**

89 The oral cavity remains an underappreciated site for SARS-CoV-2 infection despite  
90 the evident myriad of oral conditions observed in COVID-19 patients, and the presence  
91 of the virus in saliva (1-6). The homeostasis of the oral cavity is maintained by saliva, an

92 extracellular fluid produced by salivary glands possessing a wealth of protective  
93 properties (7). Specifically, saliva is enriched with antimicrobial peptides considered to be  
94 part of the host Th17-type adaptive immune response that play a vital role in innate  
95 immune defenses against microbial species (7-10). Most notable are histatins, a family of  
96 peptides exclusively produced in the acinar cells of the salivary glands and secreted into  
97 saliva (11, 12). There are two genes for histatins, *HTN1* and *HTN3* which encode  
98 histatins-1 and 3, respectively (13). Histatin-5, a proteolytic product of histatin-3, is the  
99 most abundant and unique as it exhibits potent antifungal activity against the fungal  
100 pathogen *Candida albicans* (*C. albicans*) (12, 14-18). Although *C. albicans* is a  
101 commensal colonizer of the oral cavity, any changes in the host microenvironment  
102 favoring its proliferation allows this opportunistic species to transition into a pathogen  
103 causing oral candidiasis (thrush) (19, 20). As a commensal colonizer of the oral mucosa,  
104 the host immune response to *Candida* is oriented toward a more tolerogenic state and,  
105 therefore, local innate immune defenses and specifically histatin-5 play a central role in  
106 maintaining *Candida* in its commensal state preventing development of oral candidiasis  
107 (8, 21, 22).

108 Recently, the salivary glands were shown to be a potential target for SARS-CoV-2  
109 infection as several studies demonstrated the concomitant expression of  
110 ACE2/transmembrane serine proteases 2 (TMPRSS2) in salivary glands epithelial cells  
111 (23-27). In fact, virus entry into salivary glands cells was found to be higher, as compared  
112 with entry into lung cells (25). Most notable are findings from a landmark study by Huang  
113 and Perez *et al.* (2021) (28) which comprehensively demonstrated that salivary gland  
114 acinar and ductal cells are robust sites for SARS-CoV-2 infection and replication, eliciting

115 local immune cell activation. Additionally, architectural distortion, atrophy, fibrosis, and  
116 ductal rupture were also revealed, establishing that the minor and major salivary glands  
117 are susceptible sites for infection, replication and local immune cell activation. Moreover,  
118 the authors demonstrated that saliva from acutely infected patients could infect and  
119 replicate in Vero cells, *ex vivo*, indicating that the source of virus in saliva is likely derived  
120 from infected cells in the salivary glands (28). In fact, clinical observations are in support  
121 of SARS-CoV-2 mediated damage to the salivary glands as COVID-19 patients frequently  
122 present with gustatory dysfunction and xerostomia, and cases of inflamed salivary glands  
123 have been reported in this population (26, 29).

124 Unlike other antimicrobial peptides, histatins are exclusively expressed and secreted  
125 by acinar cells of salivary glands; saliva containing histatins is secreted from the acini into  
126 the lumen which transits the ductal network into the oral cavity where they can exert their  
127 antimicrobial activities. Patients infected with SARS-CoV-2 have the propensity to  
128 develop superimposed infection including oral candidiasis. While SARS-CoV-2 infects  
129 and replicates in the acinar and ductal cells of the salivary glands, it is not known if the  
130 risk of oral candidiasis is due to affects on the acinar expression of anti-candidal proteins,  
131 or due to viral and immune-mediated destruction of the glands. To that end, we performed  
132 mechanistic and clinical studies to investigate the implications of SARS-CoV-2 infection  
133 of salivary gland tissue on oral innate immune defenses, salivary histatin-5 production,  
134 and predisposition to opportunistic infections. Using *in situ* hybridization and  
135 immunofluorescence, we performed co-localization studies to assess histatin production  
136 in SARS-CoV-2 infected salivary gland acinar cells. To provide mechanistic insights, the  
137 expression of histatin genes was comparatively evaluated in infected and uninfected

138 salivary gland tissue. The clinical implications of findings from mechanistic studies were  
139 demonstrated using various cohorts of SARS-CoV-2 infected subjects to evaluate salivary  
140 histatin-5 levels and oral *Candida* colonization. Collectively, the novel findings from this  
141 study establish the oral cavity as a robust site for SARS-CoV-2 infection warranting  
142 reassessment of the risks for oral opportunistic infections in COVID-19 patients.

143

## 144 **RESULTS**

145 **SARS-CoV-2 infection of the parotid glands affects the expression of histatins.** To  
146 determine the effect of SARS-CoV-2 infection on the expression of anti-candidal proteins  
147 in the salivary glands, RNA sequencing (RNAseq) and confirmatory hybrid *in situ*  
148 hybridization and immunofluorescence microscopy, was used. First, RNAseq of SARS-  
149 CoV-2 infected parotid glands showed significantly reduced expression of histatin genes  
150 (*HTN1*, >100-fold lower,  $p=0.0022$ ; *HTN3*, >100-fold lower,  $p=0.0038$ ; Fig. 1a). Next, we  
151 confirmed the loss of histatin expression and the co-localization of SARS-CoV-2 and  
152 histatin protein expression in acinar cells. Hybrid *in situ* hybridization and  
153 immunofluorescence microscopy co-localization studies of SARS-CoV-2 and histatins,  
154 respectively, demonstrated significant ( $p<0.001$ ) reduction of histatin protein expression  
155 in virus infected acinar cells in parotid gland tissues obtained from deceased COVID-19  
156 patients. As previously reported, the detection of SARS-CoV-2 is non-uniform across the  
157 acini of the glands (28). Comparing infected vs non-infected acinar cells, histatin protein  
158 expression intensity was inversely proportional to viral count (Fig.1b-f) indicating that  
159 direct viral infection of the glands suppresses histatin mRNA and protein expression.

160

161 **SARS-infected patients secrete significantly less histatins potentiating oral**  
162 **candidiasis.** Clinical studies were conducted using two COVID-19 patient cohorts  
163 (hospitalized [UMD] and outpatient [NIDCR]) with ranging disease severity, and matched  
164 healthy controls. In the hospitalized cohort, a histatin-5 specific immunoassay to measure  
165 salivary histatin-5 concentrations was used and significant ( $p=0.0303$ ) differences in  
166 values between the COVID-19 patients and matched healthy controls were seen. Average  
167 concentrations for the control group was  $21.3 \mu\text{g/ml}$  ( $11.1 \mu\text{g/ml}$ - $34.5 \mu\text{g/ml}$ ), and  $18.4 \mu\text{g/ml}$   
168 ( $1.4 \mu\text{g/ml}$ - $53.5 \mu\text{g/ml}$ ) for the COVID-19 group. Strikingly, 14 of the COVID-19  
169 patients had concentrations below  $10 \mu\text{g/ml}$  (Fig. 2a), and although unclear why, 3  
170 subjects had concentrations higher than any of the controls. The difference in  
171 concentrations between the two groups was also seen in age- and race-matched  
172 comparison between each COVID-19 patient and their matched control subject (Fig. 2b).  
173 *Candida* colonization was assessed by culturing samples; where no *Candida* was  
174 recovered from any of the healthy controls, 45% (9/20) of COVID-19 patients sampled  
175 were positive for *C. albicans*, some heavily colonized (Fig. 2a).

176 To corroborate these findings, a separate outpatient cohort collected by the  
177 National Institute of Dental and Craniofacial Research (NIDCR) (28) of serially sampled  
178 acutely infected patients was analyzed for histatin-5 expression. Compared to healthy  
179 control samples collected prior to the pandemic ( $n=9$ ), the acute phase COVID-19 whole  
180 unstimulated saliva ( $n=23$ ) had significantly lower histatin-5 concentrations ( $3.63 \mu\text{g/ml}$  vs  $10.41 \mu\text{g/ml}$ ,  $p<0.0001$ ; Fig. 2c). *Candida* colonization was assessed as above; no *Candida* was  
181 recovered from the healthy controls, yet 17% (4/23) of COVID-19 patients sampled were  
182 positive for *C. albicans*. Despite high variability in the expression of histatin-5 across the  
183

184 cohort, prospective analysis of available serially-collected samples (n=8; 3-15 days from  
185 symptom onset, 6-months, and 1-year from initial infection) from these COVID-19  
186 subjects indicated a slight, but statistically significant trend in the restoration histatin-5  
187 concentration from the post-acute to the chronic phase ( $R^2=0.30$ ,  $p=0.0046$ ; Fig. 2d).  
188 However, some patients exhibited persistence of low salivary histatin concentration for up  
189 to 1 year after recovery in the chronic phase. No statistical differences (p values > 2.0) in  
190 histatin-5 concentrations were seen between subjects based on disease severity or other  
191 variables (gender, race, age).

192 **Significant changes in histatin-5 concentrations over the course of COVID-19**  
193 **disease in prospectively sampled subjects.** A total of 5 subjects with mild-moderate  
194 disease were prospectively sampled and salivary histatin-5 was measured to monitor  
195 changes in concentrations. Two of the subjects were longitudinally sampled up to 39 and  
196 80 days, respectively (Fig. 3). For these subjects, saliva and histatin-5 concentrations  
197 prior to COVID-19 infection were available. The baseline histatin-5 concentration  
198 measured prior to COVID-19 disease for *Subject #1* was 15.7  $\mu$ g/ml. However, the  
199 concentration in the first sample recovered during the acute phase of the disease was 5.6  
200  $\mu$ g/ml (64.33% drop) and 8.8  $\mu$ g/ml for the second sample recovered 2 days later. The  
201 concentration gradually began to increase during the post-acute phase with a spike noted  
202 on Day 15 (25.3  $\mu$ g/ml) returning to baseline level in the last sample analyzed (Fig. 3a).  
203 For *Subject #2*, the histatin-5 concentration measured prior to COVID-19 disease was  
204 32.8  $\mu$ g/ml; however, the concentration in the first sample recovered during the post-acute  
205 phase of the disease was 15.65  $\mu$ g/ml (52.29% drop) which gradually increased over  
206 subsequent days with a spike noted on Day 45 (43.6  $\mu$ g/ml) before returning to pre-

207 COVID-19 levels on last day sampled (Fig. 3c). Significantly, *C. albicans* was recovered  
208 from the initial 6 samples recovered from *Subject #2*, but not from the last 3 samples that  
209 followed the restoration of histatin-5 to pre-COVID-19 level (Fig. 3c). Three additional  
210 subjects (Subjects 3, 4, and 5) were also prospectively sampled (Fig. 4), however, for this  
211 group, pre-COVID-19 saliva was not available. For these subjects, the histatin-5  
212 concentrations in the first samples recovered during the acute phase of the disease were  
213 2.4, 4.1 and 5.6  $\mu$ g/ml, respectively which increased during the post-acute phase to 10.9,  
214 13.2, and 12.5  $\mu$ g/ml, respectively in the last samples tested (Fig. 4). No *Candida* was  
215 recovered from any of the samples from these 3 subjects.

216 **Activation of Th17 inflammatory pathway concomitant with changes in histatin-5**  
217 **concentrations.** Salivary cytokine profiling was performed on samples recovered from  
218 the 5 prospectively sampled subjects. Comparative analysis of samples from *Subject #1*  
219 demonstrated a notable increase in the Th17 associated inflammatory cytokines;  
220 compared to baseline pre-COVID-19 sample (IL-17A, IL-17F, IL-6, IL-10, TNF- $\alpha$ , IFN- $\gamma$ ,  
221 IL-22, GMCSF and IL-23); concentrations gradually increased with a spike on Day 15,  
222 decreasing over subsequent days and returning to baseline level in the last sample  
223 measured (Day 39) (Fig. 3b). Although IL-1 $\beta$  followed the same trend, the spike in  
224 concentration was seen in the first sample recovered during the acute phase of the  
225 disease. Cytokine levels in *Subject #2* similarly demonstrated an increase in the Th17  
226 associated inflammatory cytokines; compared to baseline pre-COVID-19 sample,  
227 concentrations of all cytokines (IL-17A, IL-17F, IL-6, IL-10, TNF- $\alpha$ , IFN- $\gamma$ , IL-22, GMCSF,  
228 IL-23 and IL-1 $\beta$ ) spiked on Day 38, gradually decreasing and returning to baseline level  
229 on Day 45. IL-17E was not detectable in all samples analyzed for *Subject #1* and *Subject*

230 #2 (Fig. 3b, 3d). For the remaining 3 subjects, increase in Th17-associated inflammatory  
231 cytokines was similarly observed during the post-acute phase for *Subject #3* (Fig. 4). Only  
232 the first and last samples recovered from these 3 subjects were subjected for cytokine  
233 analysis.

234 **C. albicans** proliferates in saliva from COVID-19 positive subjects with low histatin-  
235 **5.** Saliva recovered from subjects (n=3) during acute COVID-19 infection (low histatin-5)  
236 and post-acute recovery (high histatin-5) phases were separately pooled and histatin-5  
237 concentrations determined. Samples were subsequently tested *in vitro* for ability to control  
238 C. albicans proliferation (Fig. 5a). Histatin-5 concentration in the pooled saliva sample  
239 obtained during acute COVID-19 was 0.5 µg/ml (low), and in the pooled sample recovered  
240 during post-recovery concentration was 11.5 µg/ml (high) (Fig. 5b). Based on C. albicans  
241 growth (CFUs) following *in vitro* inoculation of saliva with 1x10<sup>4</sup> cells/ml C. albicans, an  
242 average of 2.55x10<sup>4</sup> cells/ml C. albicans was recovered from the low histatin-5 sample  
243 and 1.29x10<sup>4</sup> cells/ml from the high histatin-5 sample (Fig. 5c).

244

## 245 **DISCUSSION**

246 To date, little is known about the physiological mechanisms of oral manifestations in  
247 COVID-19 disease and the impact of SARS-CoV-2 infection on salivary gland function.  
248 Clinical observations are in support of SARS-CoV-2 mediated damage to the salivary  
249 glands, as COVID-19 patients frequently present with gustatory dysfunction  
250 and xerostomia, and clinical cases of inflamed salivary glands have been reported in this  
251 patient population (26).

252 Oral candidiasis is the most common opportunistic infection, particularly in  
253 immunocompromised individuals, although immunocompromise due to COVID-19 is  
254 ardently debated (1). However, the onset of oral candidiasis early in HIV disease indicates  
255 that immunity to *Candida* is site-specific and involves secondary local innate defenses  
256 (21, 22). In fact, innate immunity not only represents the first line of defense providing the  
257 initial host response to pathogens, but also activates the adaptive immunity (8). These  
258 systems exhibit coordinated regulation and response to establish and maintain tissue  
259 homeostasis (8). Host-produced salivary antimicrobial peptides are considered to play a  
260 vital role in innate immune defenses against microbial species, specifically histatins which  
261 are localized in the serous acinar cells and secreted into saliva (7, 12, 14).

262 The recent demonstration of SARS-CoV-2 replication in salivary glands and  
263 destruction of gland integrity including at sites where histatins are produced. These  
264 findings indicate that histatin production may be compromised in infected individuals. This  
265 hypothesis was validated using transcriptional analysis where the expression of both  
266 histatin genes (*HTN1* and *HTN3*) were shown to be downregulated in SARS-CoV-2  
267 infected salivary gland tissue (Fig. 1a). Importantly, SARS-CoV-2 and histatin co-  
268 localization studies indicated an inversely proportional association where little or no  
269 histatin signal was detected in virus infected acinar cells compared to uninfected cells  
270 (Fig. 1b-f). The clinical implications of these findings were subsequently revealed using  
271 various cohorts of SARS-CoV-2 infected subjects. Overall, analysis of saliva samples  
272 demonstrated significant reduction in histatin-5 levels in infected subjects compared to  
273 healthy controls (Fig. 2). However, despite an association between infection and reduced  
274 histatin expression, the exact temporal relationship could not be perfectly gleaned. To

275 better understand the temporal relationship between infection and histatin expression, we  
276 included a panel of prospective samples from moderately symptomatic COVID-19  
277 subjects, which allowed us to glean some insights (Fig. 3, 4). Specifically, analysis  
278 indicated that the decrease in histatin-5 during COVID-19 is likely reversible as  
279 concentrations tended to increase during the post-acute phase of the disease. However,  
280 it is important to iterate that co-localization studies exhibited an inversely proportional  
281 association between histatin and viral counts in infected acinar cells (Fig. 1c-f), and some  
282 patients experienced long-term deficits in salivary histatin-5 levels (42 days to 1 year).  
283 Therefore, in severe COVID-19, a robust salivary infection and the ensuing adaptive  
284 immune response may irreparably damage the salivary gland parenchyma. Thus, due to  
285 pathologically lower histatin-5 secretion (and likely reduced saliva secretion overall),  
286 affected individuals may remain predisposed to both recurrent and recalcitrant to  
287 antifungal therapy oral candidiasis as part of the Long COVID syndrome (30)  
288 (<https://www.covid.gov/be-informed/longcovid/about#term>). It is important to note here  
289 that there are no known set “*normal*” values for salivary histatin-5 concentrations and  
290 what is considered physiological is dependent on many factors including: host factors  
291 (e.g, age, sex), time of collection, the collection method, and post-processing. Moreover,  
292 histatin-5 expression is secreted primarily by serous acinar cells; these cells  
293 predominate in the parotid glands but are half the acinar cells in the submandibular  
294 glands, and almost entirely absent from the sublingual glands. The relative contributions  
295 of each gland to the total saliva collected is also host specific. Therefore, it is expected to  
296 see a wide range of histatin-5 concentrations among the healthy control subjects.  
297 However, based on our experience using our assay, prior clinical studies, and evaluations

298 of anti-candidal activity, we have set arbitrary concentrations as a general guidelines for  
299 what is physiological (31).

300 With limited available clinical information on the hospitalized cohort population  
301 (including presence of oral lesions), we recognize that we cannot fully account for  
302 confounding factors that may influence histatin-5. However, our study focuses on the  
303 presence of SARS-CoV-2 virus rather than disease severity; importantly, on average we  
304 observed lower histatin-5 levels for infected subjects in all cohorts studied (hospitalized,  
305 outpatient and individual case). In our analysis, we did not find strong association  
306 between histatin-5 concentrations and *Candida* colonization regardless of disease status  
307 or demographics. One intriguing observation in the samples from the hospitalized cohort  
308 is the exceptionally high histatin-5 concentrations seen for 3 of the subjects with values  
309 higher than that of any of the healthy controls (Fig. 2a). Although unclear as to why, it is  
310 important to note that in the two prospectively sampled subjects with known pre-COVID-  
311 19 histatin-5 values, a spike in histatin-5 and inflammatory cytokines was noted over the  
312 course of the disease progression prior to return to baseline levels (Fig. 3). Therefore, we  
313 speculate that these three hospitalized subjects may have been sampled during these  
314 transient spikes. Interestingly, all 3 subjects with high histatin-5 levels were also positive  
315 for *C. albicans* (Fig. 2a), and it is tempting to also speculate that these high values may  
316 be part of the host immune response to *Candida* presence.

317 Importantly, our findings demonstrated that changes in histatin-5 concentrations were  
318 concomitant with activation of the Th17 inflammatory pathway. Antimicrobial peptides,  
319 including histatins, are part of the host Th17-type adaptive immune response (8).  
320 Interleukin-17 (IL-17) is a pro-inflammatory cytokine that regulates multiple immune

321 events (32). In the tissues of the oral cavity, including the salivary glands, the IL-17/Th17  
322 signaling pathway is essential for host protection against *C. albicans* infection (32, 33).  
323 Therefore, it was not surprising that cytokine profiling of saliva samples from prospectively  
324 sampled subjects displayed a trend for the Th17 associated cytokines similar to that for  
325 histatin-5 (Fig. 3). Interestingly, in the subject heavily colonized with *C. albicans*, the spike  
326 in cytokine concentrations coincided with increase in salivary histatin-5, and more  
327 significantly, with the clearance of *C. albicans* (Fig. 3c). The activation of the Th17 immune  
328 response in COVID-19 disease is expected as immunophenotyping and microscopic  
329 analysis of SARS-CoV-2 infected salivary gland tissues demonstrated chronic, focal  
330 lymphocytic sialadenitis with a T-lymphocytic infiltrates (28, 29). As IL-17 antifungal  
331 activity involves regulation of the expression of antimicrobial peptides, including histatins  
332 (8, 32, 33), the gradual increase in histatin-5 concomitant with clearance of *C. albicans*  
333 may also be mediated by activation of Th17 response. Therefore, based on these  
334 collective findings, we presume that decreased histatin-5 salivary levels due to SARS-  
335 CoV-2 infection of salivary gland serous acini permits proliferation of colonizing *C.*  
336 *albicans* leading to the development of oral candidiasis.

337 The importance of salivary histatin-5 in controlling the proliferation of *C. albicans* was  
338 shown using an *ex vivo* anti-candidal assay where saliva with low histatin-5 was able to  
339 allow *C. albicans* proliferation *in vitro* (Fig. 5). These findings provide experimental  
340 evidence establishing the importance of salivary histatin-5 in preventing *Candida*  
341 proliferation by maintaining colonizing *Candida* in the commensal state. Further, in  
342 addition to anti-candidal activity, given the established anti-inflammatory and wound  
343 healing properties of histatins (34-36), it is possible that compromised levels of histatins

344 (and other antimicrobial proteins) may contribute to other immune- and dysbiosis-  
345 mediated mucosal conditions observed in COVID-19 patients such as burning mouth,  
346 blisters and non-specific ulcerations, and aphthous-like lesions, all of which have been  
347 associated with COVID-19 (5). With the current lack of knowledge on the implications of  
348 SARS-CoV-2 infection on oral health, the findings from this study provide mechanistic  
349 insights underscoring the oral cavities' diverse susceptibilities to SARS-CoV-2 infection,  
350 prompting a reassessment of oral opportunistic infection risks and their potential long-  
351 term impacts on oral health.

352

## 353 **METHODS**

354 **Co-localization of SARS-CoV-2 and histatin in salivary gland tissue using *in situ***  
355 **hybridization and immunofluorescence, respectively.** To investigate the expression  
356 of histatin during SARS-CoV-2 infection, we employed the RNAscope Multiplex  
357 Fluorescent v2 assay with antigen co-detection, adhering to the manufacturer guidelines.  
358 Studies were performed on parotid FFPE (formalin-fixed, paraffin-embedded) biopsies  
359 from uninfected donors (n=4) and from COVID-19 subjects (n=8) at autopsy with high and  
360 low copy virus number. Uninfected donors were procured from the Human Cooperative  
361 Tissue Network, and COVID-19 autopsy tissues were procured by the National Institutes  
362 of Health COVID-19 Autopsy Consortium, as described previously (28, 37). Initially, slides  
363 were dried in an air oven at 60°C for 30 min and subsequently rehydrated, and target  
364 retrieval was performed using 1X Co-Detection Target Retrieval for 20 min at 99°C. Slides  
365 were then rinsed briefly in water and washed in PBS-T (1X PBS, 0.1% Tween-20, pH 7.2),  
366 and a hydrophobic barrier was established using an ImmEdge pen. Primary antibodies

367 against histatin-3 (Biorbyt; diluted 1:300 in Co-detection Antibody Diluent from ACD) and  
368 AQP5 (SantaCruz; diluted 1:300 in Co-detection Antibody Diluent from ACD) were applied  
369 and slides were incubated overnight at 4°C. Following washing in PBS-T, tissues and  
370 antibodies were fixed in 10% Neutral Buffered Formalin (NBF) for 30 min at room  
371 temperature, followed by another wash in PBS-T. Tissue sections were then treated with  
372 RNAscope Protease Plus for 30 min at 40°C and immediately followed by probe  
373 hybridization using either a positive control probe (320861), negative control probe  
374 (320871), or the V-nCoV2019-S probe (848561). The V-nCoV2019-S probe is antisense  
375 and specifically targets the spike protein sequence of viral RNA, providing insights into  
376 infection and viral load within the tissue. Following hybridization, signals were amplified  
377 and visualized using fluorescence Tyramide signal amplification. The primary antibodies  
378 were detected using secondary antibodies conjugated to AF488 (histatin-3), and AF568  
379 (AQP5; aquaporin-5) and counterstaining was performed with DAPI. Images were  
380 captured using a Zeiss Axio Scan Z1 slide scanner light microscope equipped with a  
381 40x/0.95 N.A. objective, and image files were imported into Visiopharm software version  
382 2017.2. We first segmented the cells using the AI app from Visiopharm, once the cells  
383 were segmented, using the APP Author function we designed an algorithm that detects  
384 the dots of ISH and counts the number of dots per cell, and quantify the mean intensity  
385 of histatin-3 per cell. The data was exported and analyzed in Prism 10. Control  
386 experiments for *in situ* hybridization and immunofluorescence studies were performed  
387 prior to sample analysis (Supp. Fig. 1).

388

389 **Bulk RNAseq analysis of salivary gland tissue.** Total RNA was extracted from  
390 RNAlater (Invitrogen)-preserved parotid gland at autopsy from uninfected donors (n=3)  
391 and COVID-19 subjects (n=8), using the RNeasy Mini (Qiagen) according to  
392 manufacturer protocols. Following standard bulk RNAseq using Illumina platform,  
393 normalized counts per million (CPM) were plotted for *HTN1* and *HTN3* and expression  
394 levels of both genes were compared.

395

396 **Study subjects.** Hospitalized cohort. Adult COVID-19 patients (n=26) hospitalized at the  
397 University of Maryland Medical Center and a matched control (age, race and gender)  
398 group of healthy volunteers (n=26) were enrolled in the study. The University of Maryland  
399 Baltimore Institutional Review Board approved this study, no patient identifiers were used  
400 and informed consent was obtained from all subjects. Inclusion criteria for control subjects  
401 included: healthy adults over 18 years of age with no history of oral candidiasis, any  
402 predisposing factors or antifungal therapy. As the premise of the study is to investigate  
403 the presence of the virus in the oral cavity regardless of disease severity, the only  
404 inclusion criteria for the COVID-19 cohort was COVID-19 positivity. Of the 26 subjects, 11  
405 were COVID-19 positive but asymptomatic and were hospitalized for other medical  
406 reasons; the remaining 15 were symptomatic with severe disease, admitted to the  
407 intensive care unit and/or receiving oxygen supplementation. The hospitalized COVID-19  
408 population included 14 males and 12 females; 15 Caucasians and 11 African American  
409 with age range of 29-76. Outpatient cohort. This cohort included 33 subjects with mild-  
410 moderate disease; a total of 68 samples were prospectively collected from these subjects  
411 at NIDCR (previously described) (28). Prospective cases. In addition to the cohorts, 5

412 otherwise healthy outpatient subjects (4 females, one male; age range 30-58) were  
413 prospectively sampled at different timepoints during the course of their COVID-19  
414 disease. A total of 29 samples were collected and analyzed for these subjects.

415

416 **Clinical Samples.** Saliva samples were collected from participating subjects using the  
417 Salivette collection system as we previously performed (31, 38). Saliva was recovered,  
418 aliquoted and immediately stored at -80°C with protease inhibitors. In addition, oral swabs  
419 of the oral mucosal tissue were recovered for culturing to evaluate *Candida* recovery. Due  
420 to inaccessibility to some patients the result of medical status, samples for fungal culturing  
421 were only obtained from 20 of the 26 hospitalized patients. For the outpatient cohort and  
422 their control subjects, whole unstimulated saliva samples were collected and processed  
423 as above.

424

425 **Evaluation of salivary *Candida* colonization.** Oral swabs from all sampled subjects  
426 were immediately cultured on fungal Yeast Peptone Dextrose (YPD) agar media (Difco  
427 Laboratories) and incubated at 35°C for 24-48 h for fungal growth evaluation. The  
428 chromogenic medium CHROMagar Candida was used for *Candida* speciation.

429

430 **Measurement of histatin-5 (Hst-5) salivary levels using ELISA.** ELISA was performed  
431 as we previously described (31). A high purity Hst-5 peptide was synthesized by  
432 GenScript and Hst-5 specific rabbit polyclonal antibody was produced by Lampire  
433 Biological Laboratories. For measurement of Hst-5 levels, a standard curve was  
434 performed with each assay using Hst-5 peptide concentrations ranging from 0.5-500

435 µg/ml. Wells of high-binding 96-well plates were coated with 100 µl of each Hst-5  
436 concentration or 1/100 dilution of saliva. Following overnight incubation at 4°C, wells were  
437 blocked with 0.1% dry milk in PBS for 1 h and anti-Hst-5 antibody (1/1000) (100 µl) was  
438 added for 1 h at 37°C. Following washing, HRP-labeled goat anti-rabbit secondary  
439 antibody (1/3000) (Abcam) was added, and plates incubated for 1 h at 37°C. Following  
440 washing, 100 µl of ABTS Peroxidase Substrate (KPL, Inc.) was added and plates  
441 incubated for 20 min until color develops. The reaction was stopped by the addition of 50  
442 µl of Stop Solution (KPL, Inc.) and optical density (OD) was measured at 405nm using a  
443 microtiter plate reader. A standard curve was plotted with each run; samples were tested  
444 in triplicate on two separate occasions and the average Hst-5 concentration calculated in  
445 µg/ml. As there are no set normal Hst-5 salivary concentrations, based on our experience  
446 with clinical studies on Hst-5 salivary levels using our immunoassay, arbitrary  
447 concentrations of approximately 9-10 µg/ml was considered the cutoff whereby lower  
448 concentrations are considered in the low range (31).

449

450 **Salivary cytokines profiling.** Saliva samples from outpatient subjects were analyzed at  
451 the University of Maryland Cytokine Core using the Luminex Multianalyte System. Each  
452 sample was measured in triplicate and results expressed in Pg/ml. Not enough saliva was  
453 available from other cohorts for cytokine analysis.

454

455 ***Ex vivo* salivary *C. albicans* inhibition assay.** In order to assess the anti-candidal  
456 potency of saliva with respect to Hst-5 concentration, saliva samples were recovered from  
457 3 subjects during COVID-19 and after recovery, then pooled to generate a COVID-19

458 positive and a COVID-19 negative sample. Hst-5 concentration in the pooled samples  
459 was pre-determined by ELISA and samples were filter-sterilized and comparatively tested  
460 for efficacy in inhibiting *C. albicans* proliferation *in vitro*. For these assays, cultures of the  
461 standard *C. albicans* SC5314 strain were grown in YPD broth (Difco Laboratories)  
462 overnight at 30°C with shaking and cells were washed and resuspended in sterile PBS  
463 (1mM). *C. albicans* cells were added to each of the saliva samples (100 µl) at final cell  
464 density of  $1 \times 10^4$  cells/ml in the wells of a 96-well microtiter plate and plates were  
465 incubated for 1 h at 37°C with shaking. Aliquots from reactions were diluted with PBS and  
466 plated on YPD agar and incubated for 24–48 h at 35°C. The number of single colonies  
467 on each plate was counted and the level of *C. albicans* proliferation was determined  
468 based on CFU counts (cells/ml).

469

470 **Statistical analysis.** Statistical analysis was performed using GraphPad Prism 10.2.1. A  
471 Wilcoxon rank-sum test was used to compare histatin-5 levels between COVID-19  
472 patients and healthy control subjects and a t-test was used to evaluate associations  
473 between histatin-5 values and patient characteristics (disease severity, *Candida*  
474 colonization, demographics). For *in vitro* assays, histatin-5 levels in pooled saliva of  
475 COVID-19 positive and negative subjects and *Candida* CFU counts were determined  
476 using the unpaired two-sample t-tests. Significance of *HTN1* and *HTN3* expression levels  
477 in parotid glands was determined using ANOVA analysis with Bonferroni correction for  
478 multiple measurement. Figures were constructed using GraphPad Prism 10.2.1 and R  
479 statistical programming software.

480

481 **ACKNOWLEDGMENT.** We would like to acknowledge the contributions of LaToya Stubbs  
482 and Kendra Petrick who enrolled subjects and organized sampling of hospitalized cohort  
483 at the University of Maryland Medical Center. We would like to thank the NIH COVID-19  
484 Autopsy Consortium (PIs-Chertow & Kleiner) for coordination and access to tissues from  
485 fatal COVID-19 cases. We give our special thanks to the members of the NIDCR  
486 Sjögren's Disease Clinical Research Team for their coordination of patients and collection  
487 of research data and tissues. Biorender.com was used to create elements of figures.

488

489 **FUNDING.** This work was funded by the National Institutes of Health (NIH), National  
490 Institute of Dental and Craniofacial Research (NIDCR), Division of Extramural Research  
491 (R21-DE031888, PI-Rizk-Jabra, Co-I-Warner). This project was also funded by the  
492 University of Maryland Baltimore, Institute for Clinical & Translational Research (ICTR)  
493 (1UL-1TR00309, PIs-M.A.J-R & P.R). Funding was also provided through the Intramural  
494 Research Programs of the NIH/NIDCR (Z01-DE000704, PI-Warner), NIH Clinical Center,  
495 and the National Institute of Allergy and Infectious Diseases (ZIA CL090070-03, PI-  
496 Chertow). This research was supported in part by the NIDCR Genomics and  
497 Computational Biology Core: ZIC DC000086.

498

499 **AUTHOR CONTRIBUTIONS.** M.A.J-R., B.M.W., A.S., T.F.M., P.R. conceived and  
500 designed this research, M.A.J-R., B.M.W. provided funding; A.A.A., T.W.W., P.P., B.M.W.  
501 performed the experiments; D.E.K, D.S.C., S.M.H., B.G., S.S., S.R., collected and  
502 processed tissues and clinical data for COVID-19 autopsies; D.E.K, S.M.H., B.G.,  
503 performed the autopsies; D.S.C. and D.E.K., led and oversaw the NIH COVID-19 Autopsy

504 Consortium; M.A.J-R., A.A.A., T.W.W., P.P., B.M.W., A.S., T.F.M., analyzed data; M.A.J-  
505 R., A.A.A., T.W.W., B.M.W. wrote the paper; B.M.W. led and oversaw the execution of NIH  
506 clinical and molecular studies supporting this work; M.A.J-R. oversaw the entire study.

507

508 **ETHICAL APPROVAL.** *NIH.* Autopsies are exempt from NIH single institutional review  
509 board (IRB), consent from families of fatal COVID-19 cases were obtained. Otherwise,  
510 NIH single IRB conducts ethical reviews for human research studies as required by  
511 Department of Health and Human Services regulations for the Protection of Human  
512 Subjects. All patients seen at the author's (B.M.W.) institute (NIH/NIDCR) reported herein  
513 provided informed consent before participation in IRB-approved research protocols (NIH  
514 IRB: 20-D-0094, NCT04348240; NIH IRB: 15-D-0051, NCT02327884). Individuals on 20-  
515 D-0094 had the option to receive a \$50 payment per visit (\$300 total) to offset the cost of  
516 travel.

517

518 **REFERENCES**

519 1. Amorim Dos Santos J, Normando AGC, Carvalho da Silva RL, De Paula RM,  
520 Cembranel AC, Santos-Silva AR, et al. Oral mucosal lesions in a COVID-19 patient: New  
521 signs or secondary manifestations? *Int J Infect Dis.* 2020;97:326-8.

522 2. Salehi M, Ahmadikia K, Badali H, Khodavaisy S. Opportunistic fungal Infections in  
523 the epidemic area of COVID-19: A clinical and diagnostic perspective from Iran.  
524 *Mycopathologia.* 2020 185(4):607-11.

525 3. Salehi M, AhmadiKia K, Mahmoudi S, Kalantari S, JamaliMoghadamsiahkali S,  
526 Izadi A, et al. Oropharyngeal candidiasis in hospitalised COVID-19 patients from Iran:  
527 Species identification and antifungal susceptibility pattern. *Mycoses*. 2020; 63(8):771-8.

528 4. Riad A, Gad A, Ockova B, Klugar M. Oral candidiasis in non-severe COVID-19  
529 patients: Call for antibiotic stewardship. *Oral Surg*. 2020;15(3): 465-466.

530 5. Amorim Dos Santos J, Normando AGC, Carvalho da Silva RL, Acevedo AC, De  
531 Luca Canto G, Sugaya N, et al. Oral manifestations in patients with COVID-19: A living  
532 systematic review. *Dent Res*. 2021;100(2):141-54.

533 6. Brandini DA, Takamiya AS, Thakkar P, Schaller S, Rahat R, Naqvi AR. Covid-19  
534 and oral diseases: Crosstalk, synergy or association? *Rev Med Virol*. 2021; 31(6): e2226.

535 7. Vila T, Rizk AM, Sultan AS, Jabra-Rizk MA. The power of saliva: Antimicrobial and  
536 beyond. *Plos Pathog*. 2019;15(11).

537 8. Salvatori O, Puri S, Tati S, Edgerton M. Innate immunity and saliva in *Candida*  
538 *albicans*-mediated oral diseases. *J Dent Res*. 2016;95(4):365-71.

539 9. Sultan AS, Kong EF, Rizk AM, Jabra-Rizk MA. The oral microbiome: A lesson in  
540 co-existence. *PLoS Pathog*. 2018;14(1):e1006719.

541 10. Peters BM, Shirtliff ME, Jabra-Rizk MA. Antimicrobial peptides: Primeval  
542 molecules or future drugs? *PLoS Pathog*. 2010;6(10):e1001067.

543 11. Oppenheim FG, Xu T, McMillian FM, Levitz SM, Diamond RD, Offner GD, et al.  
544 Histatins, a novel family of histidine-rich proteins in human parotid secretion. *J Biol Chem*.  
545 1988;263(16):7472-7.

546 12. Ahmad M, Piludu M, Oppenheim FG, Helmerhorst EJ, Hand AR.  
547 Immunocytochemical localization of histatins in human salivary glands. *J Histochem*  
548 *Cytochem*. 2004;52(3):361-70.

549 13. Sabatini L, Azen E. Two coding change mutations in the HIS2(2) allele characterize  
550 the salivary histatin 3-2 protein variant. *Human Mutation*. 1994;4(1):12-9.

551 14. Edgerton M, Koshlukova SE, Araujo MWB, Patel RC, Dong J, Bruenn J. Salivary  
552 histatin 5 and human neutrophil defensin 1 kill *Candida albicans* via shared pathways.  
553 *Animicrob Agents Chemother*. 2000;44(12):3310-6.

554 15. Edgerton M, Koshlukova S, Lo T, Chrzan B, Straubinger R, Raj P. Candidacidal  
555 activity of salivary histatins. *J Biol Chem*. 1998;272(32):20438-47.

556 16. Helmerhorst EJ, Troxler RF, Oppenheim FG. The human salivary peptide histatin  
557 5 exerts its antifungal activity through the formation of reactive oxygen species. *Proc Nat*  
558 *Acad Sci*. 2001;98(25):14637-42.

559 17. Nikawa H, Jin C, Fukushima H, Makihira S, Hamada T. Antifungal activity of  
560 histatin-5 against non-albicans *Candida* species. *Oral Microbiol Immunol*. 2001;16:250-  
561 2.

562 18. Situ H, Bobek L. In vitro assessment of antifungal therapeutic potential of salivary  
563 histatin-5, two variants of histatin-5, and salivary mucin (MUC7) domain 1. *Animicrob*  
564 *Agents Chemother* 2000;44(6):1485-93.

565 19. Jabra-Rizk MA, Kong E, Tsui C, Nguyen M, Clancy C, Fidel P, et al. *Candida*  
566 *albicans* pathogenesis: Fitting within the host-microbe damage response framework.  
567 *Infect Immun*. 2016;84(10):2724-39.

568 20. Vila T, Sultan AS, Montelongo-Jauregui D, Jabra-Rizk MA. Oral candidiasis: A  
569 disease of opportunity. *J Fungi (Basel)*. 2020;6(1):pii: E15.

570 21. Fidel PJ. Immunity to *Candida*. *Oral Dis*. 2002;8(Suppl 2):69-75.

571 22. Fidel PL, Jr. *Candida*-host interactions in HIV disease: Relationships in  
572 oropharyngeal candidiasis. *Adv Dent Res*. 2006;19:80-4.

573 23. Song J, Li Y, Huang X, Chen Z, Li Y, Liu C, et al. Systematic analysis of ACE2  
574 and TMPRSS2 expression in salivary glands reveals underlying transmission mechanism  
575 caused by SARS-CoV-2. *J Med Virol*. 2020;92(11):2556-66.

576 24. da Silva Pedrosa M, Sipert CR, Nogueira FN. Are the salivary glands the key  
577 players in spreading COVID-19 asymptomatic infection in dental practice? *J Med Virol*.  
578 2021;93(1):204-5.

579 25. Pascolo L, Zupin L, Melato M, Tricarico PM, Crovella S. TMPRSS2 and ACE2  
580 coexpression in SARS-CoV-2 salivary glands infection. *J Dent Res*. 2020;99(10):1120-1.

581 26. Corchuelo J, Ulloa FC. Oral manifestations in a patient with a history of  
582 asymptomatic COVID-19: Case report. *Int J Infect Dis*. 2020;100:154-7.

583 27. Tsuchiya H. Oral symptoms associated with COVID-19 and their pathogenic  
584 mechanisms: A literature review. *Dent J (Basel)*. 2021;9(3):32.

585 28. Huang N, Pérez P, Kato T, al. e. SARS-CoV-2 infection of the oral cavity and saliva.  
586 *Nat Med* 2021;27(5):892-903.

587 29. Shen Y, Voigt A, Goranova L, Abed M, Kleiner DE, Maldonado JO, et al. Evidence  
588 of a Sjögren's disease-like phenotype following COVID-19 in mice and humans. *JCI*  
589 *Insight*. 2023;8(24):e166540.

590 30. Pisano M, Romano A, Di Palo MP, Baroni A, Serpico R, Contaldo M. Oral  
591 candidiasis in adult and pediatric patients with COVID-19. *Biomedicines*.  
592 2023;11(13):846.

593 31. Khan SA, Fidel Jr P, Al Thunayyan A, Meiller T, Jabra-Rizk MA. Impaired histatin-  
594 5 level and salivary antimicrobial activity against *C. albicans* in HIV-infected individuals. *J*  
595 *AIDS Clin Res*. 2013;4(2):1-6.

596 32. Gaffen SL, Moutsopoulos NM. Regulation of host-microbe interactions at oral  
597 mucosal barriers by type 17 immunity. *Sci Immunol*. 2020;5(43):eaau4594.

598 33. Pavlova A, Sharafutdinov I. Recognition of *Candida albicans* and role of innate  
599 type 17 immunity in oral candidiasis. *Microorganisms*. 2020;8(9):1340.

600 34. Kong E, Tsui C, Boyce H, Ibrahim A, Hoag S, Karlsson A, et al. Development and  
601 *in vivo* evaluation of a novel histatin-5 bioadhesive hydrogel formulation against oral  
602 candidiasis. *Antimicrob Agents Chemother*. 2015;60(2):881-9.

603 35. Sultan AS, Rizk AM, Vila T, Ji Y, Masri R, Jabra-Rizk MA. Digital design of a  
604 universal rat intraoral device for therapeutic evaluation of topical formulation against  
605 *Candida*-associated denture stomatitis *Infect Immun*. 2019 87(12):e00617-19.

606 36. Sultan AS, Vila T, Hefni E, Karlsson AJ, Jabra-Rizk MA. Evaluation of the antifungal  
607 and wound healing properties of a novel peptide-based bioadhesive hydrogel formulation.  
608 *Antimicrob Agents Chemother*. 2019;63(10):e00888-19.

609 37. Stein SR, Ramelli SC, Grazioli A, Chung JY, Singh M, Yinda CK, et al. SARS-CoV-  
610 2 infection and persistence in the human body and brain at autopsy. *Nature Biotech*.  
611 2022;612(7941):758-63.

612 38. Alfaifi A, Sultan A, Montelongo-Jauregui D, Meiller TF, Jabra-Rizk MA. Long-term  
613 post-COVID-19 associated oral inflammatory sequelae. *Front Cell Infect Microbiol.*  
614 2022;12:831744.

615

616 **FIGURE LEGEND**

617

618 **Figure 1. Impact of SARS-CoV-2 salivary gland infection on histatin production,**  
619 **gene expression and salivary levels.** (a) Parotid expression of histatin genes (*HTN1*  
620 and *HTN3*) from deceased COVID-19 subjects (n=8) and healthy control subjects (n=3)  
621 using bulk RNA sequencing. (b-f) Co-localization studies using *in situ* hybridization for  
622 SARS-CoV-2 (*white dots and arrows*) and immunofluorescence for histatin-3 (*green*) with  
623 quantitative correlation between the intensity of histatin and SARS-CoV-2 counts within  
624 infected acinar cells of parotid tissue from (b) healthy subject (*white asterisk*, non-specific  
625 signal) and (c, e) deceased COVID-19 patients. Acini (dotted circles) identified based on  
626 expression of AQP5 (*red*, apical membrane); *inset* (*orange box*) shows the presence of  
627 the viral genome in acinar cells of the parotid glands. (d, f) Per acinar cell expression of  
628 histatin and the per cell viral count are inversely proportional as shown in two  
629 representative COVID-19 cases (P7, P19).

630

631 **Figure 2. Salivary histatin-5 (Hst-5) levels and fungal colonization in prospectively**  
632 **sampled hospitalized and outpatient COVID-19 cohorts.** (a) Boxplot with Hst-5  
633 concentrations and *Candida* recovery from 26 saliva samples from hospitalized COVID-  
634 19 patients and matched healthy controls. (b) Waterfall plot depicting 26 pairs of COVID-

635 19 and healthy subjects matched for race and age. Bar height represents differences  
636 among pairs in Hst-5 levels ( $\mu\text{g/ml}$ ) between healthy controls and COVID-19 patients. **(c)**  
637 Bar plot depicts Hst-5 concentrations and *Candida* recovery of 9 healthy subjects and 23  
638 COVID-19 outpatients' saliva. Red marked dots indicate cultured saliva contained  
639 candidal outgrowth **(d)** Linear regression analysis of serially sampled COVID-19  
640 outpatients' saliva ( $n=8$ ) shows time-dependent restoration of Hst-5 concentration from  
641 the post-acute phase to the chronic phase, based on longitudinally collected samples  
642 from acute phase (3-15 days) to chronic phase (6-12 months). Blue line, linear fit; light  
643 blue shading, confidence interval of the linear fit.

644

645 **Figure 3. Prospective time course longitudinal analysis of saliva samples for Hst-5**  
646 **from two subjects with moderate COVID-19.** Changes in Hst-5 and cytokine  
647 concentrations in two longitudinally sampled subjects prior to and during the acute and  
648 post-acute phases of COVID-19 disease. Timeline of sampling during COVID-19 infection  
649 up to 49 and 85 days post-COVID-19 infection for subjects 1 and 2 **(a and c,**  
650 **respectively).** Measurement of Hst-5 concentrations and fungal culturing of samples  
651 from the two subjects prior to and during the acute and post-acute phases of COVID-19  
652 disease. Line graphs in bottom rows depict similar trends for Hst-5 and Th17 associated  
653 cytokine levels for subjects 1 and 2 **(b and d, respectively).** Upon culturing, *C. albicans*  
654 was recovered from the initial 6 samples from subject 2 **(c, d).**

655

656 **Figure 4. Prospective sampling and analysis of saliva from three subjects with**  
657 **moderate COVID-19.** Timeline of sampling and measurement of salivary Hst-5 and

658 cytokine concentrations in samples recovered during the acute phase of the disease and  
659 upon recovery. Table presents cytokine values measured in the first and last samples  
660 recovered from the three subjects and the percent change in levels between the samples.

661

662 **Figure 5. *Ex vivo* proliferation assay using pooled saliva. (a)** Workflow for histatin-5  
663 measurement and proliferation assay using pooled saliva samples from 3 subjects under  
664 a COVID-19 infected state (PC+) and recovered state (PC-). **(b)** Bar plots depict Hst-5  
665 concentrations ( $\mu\text{g/ml}$ ) from pooled saliva samples; **(c)** recovered *C. albicans* (cells/ml)  
666 following 1 h incubation in pooled saliva samples seeded with  $1 \times 10^4$  cells/ml of *C.*  
667 *albicans*.

668

669

## 670 **SUPPLEMENTAL FIGURES**

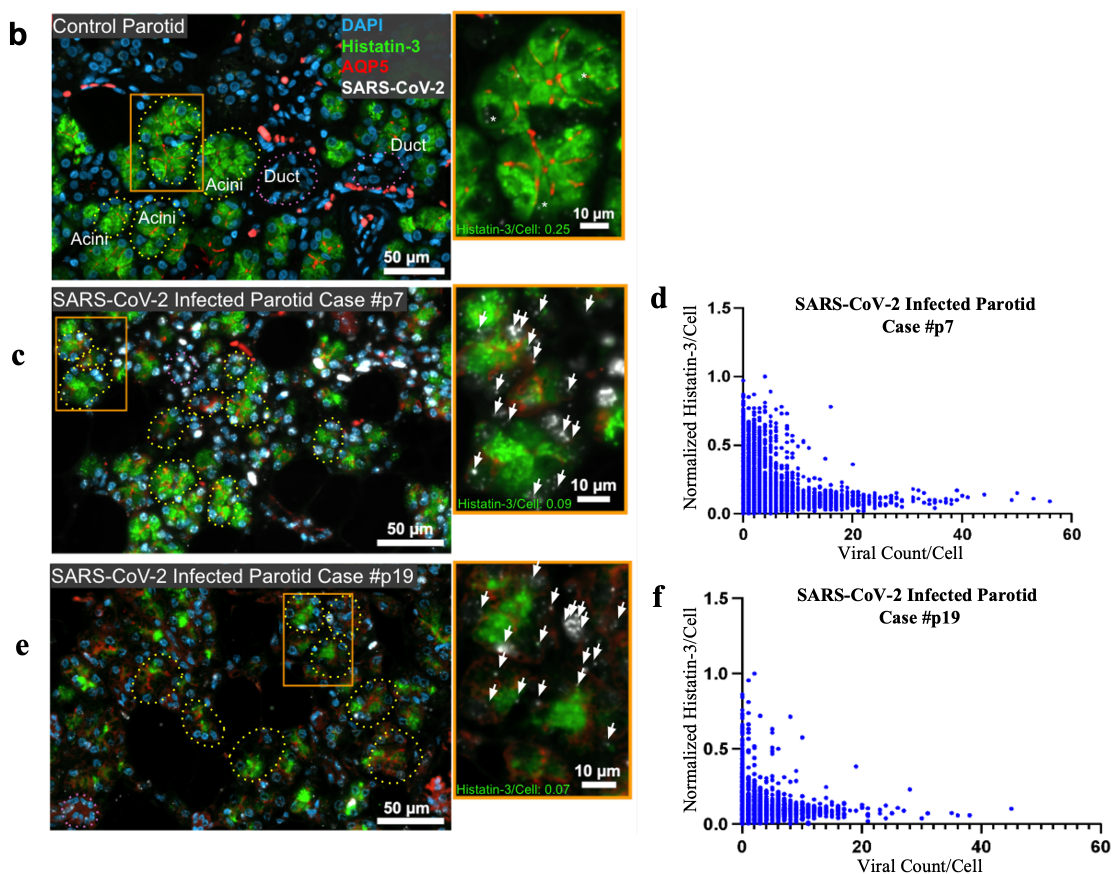
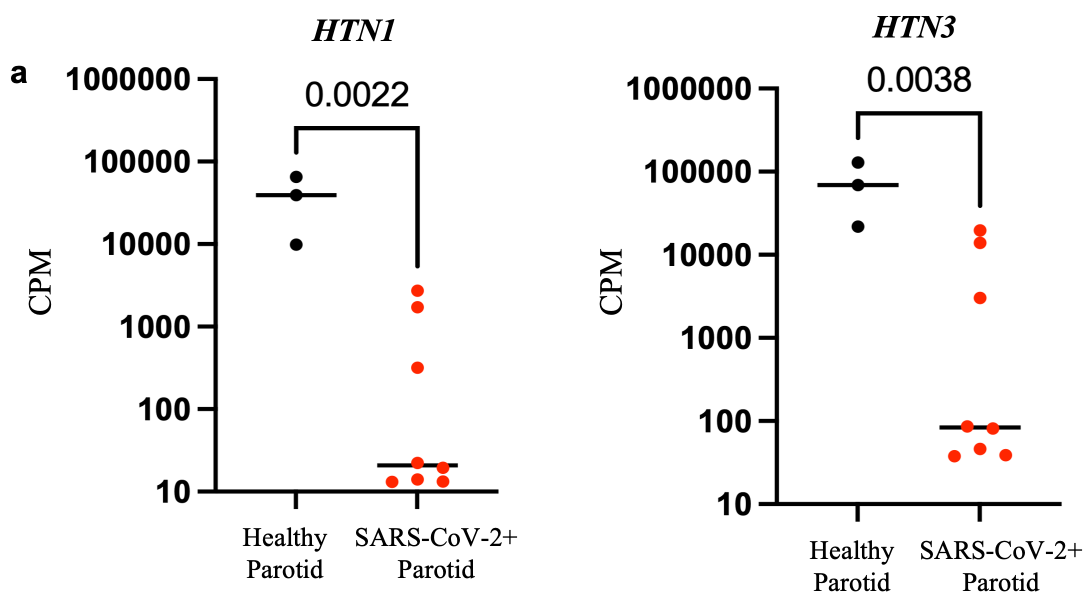
671

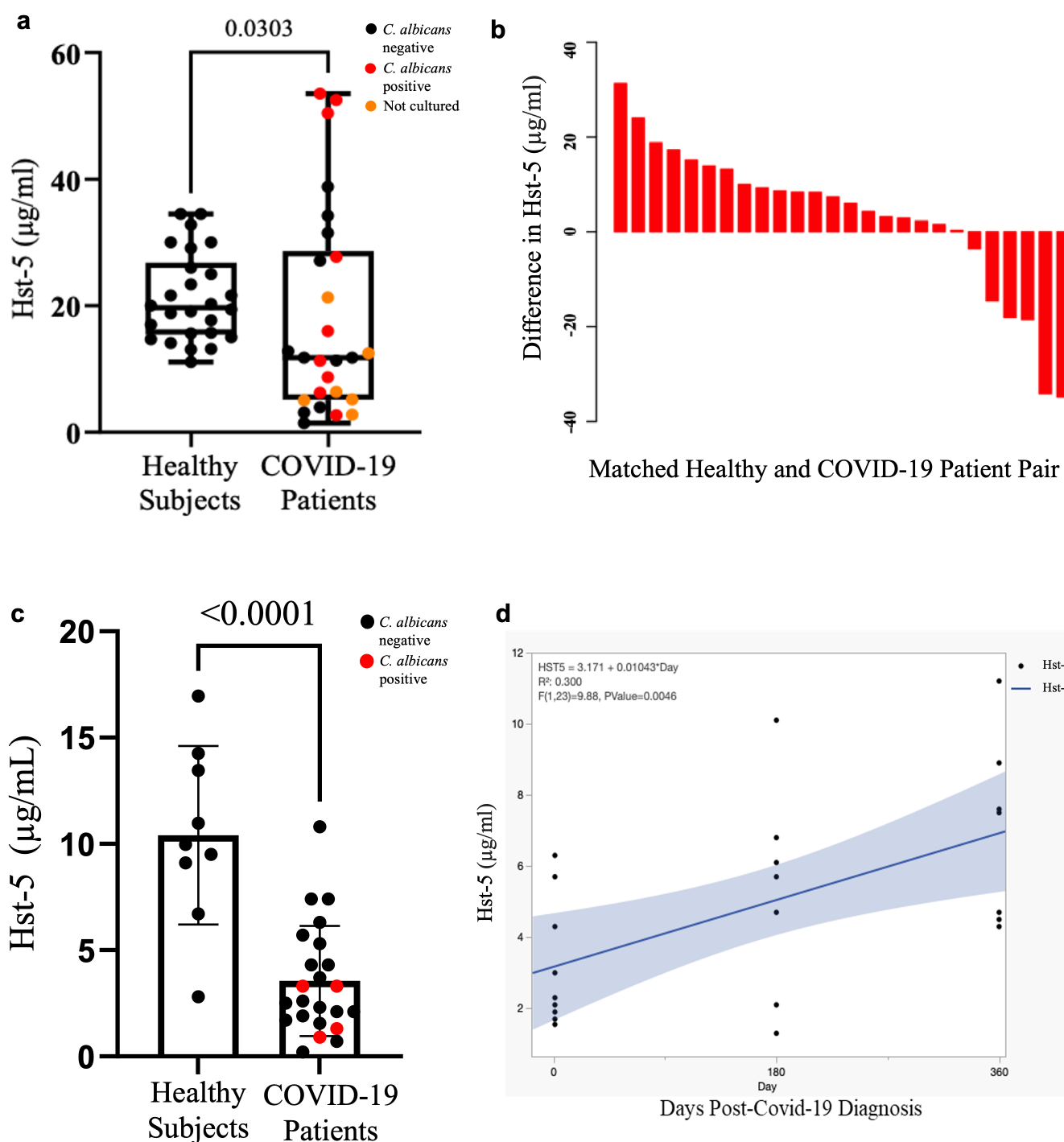
672 **Supp Figure 1. *In situ* hybridization and immunofluorescence controls. (a)**  
673 Immunofluorescence (IF) and *in situ* hybridization (ISH) controls (see also **Fig. 1**).  
674 Positive and negative controls for IF, antibody anti-Hst-3 in control parotid shows strong  
675 IF (green) in acini structures and no signal is observed in ducts. The isotype control shows  
676 no signal. **(b)** Probe anti-human *PPIB* shows strong signal in all the cells (white); negative  
677 control probe shows sparse, rare positive signal in the tissue.

678

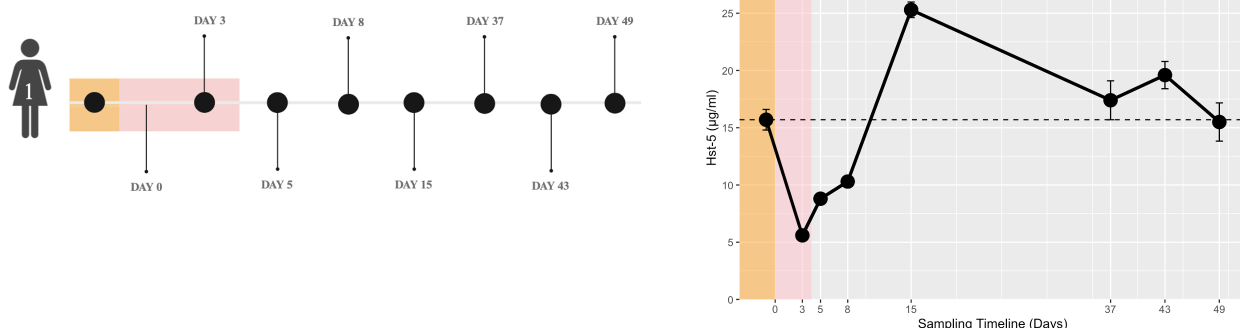
679

680

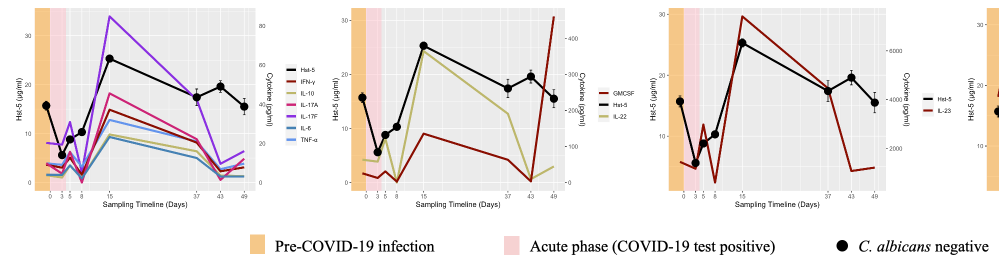




**a**

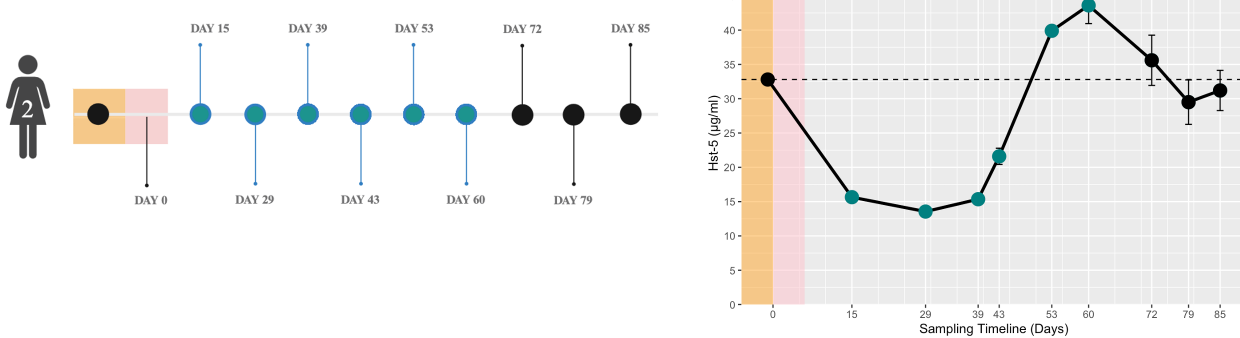


**b**

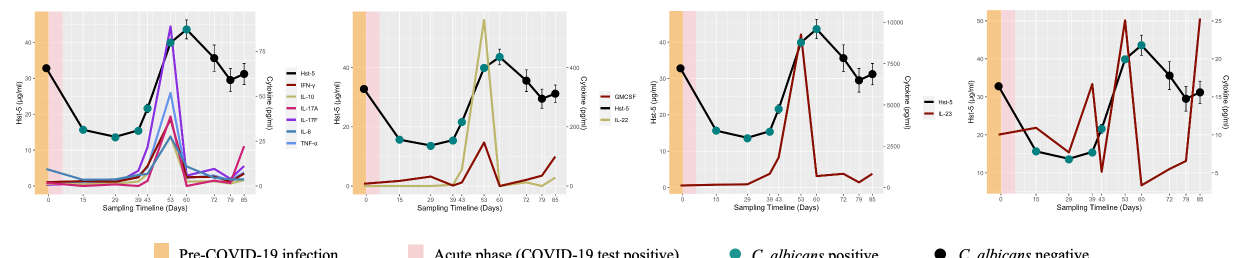


■ Pre-COVID-19 infection ■ Acute phase (COVID-19 test positive) ■ C. albicans negative

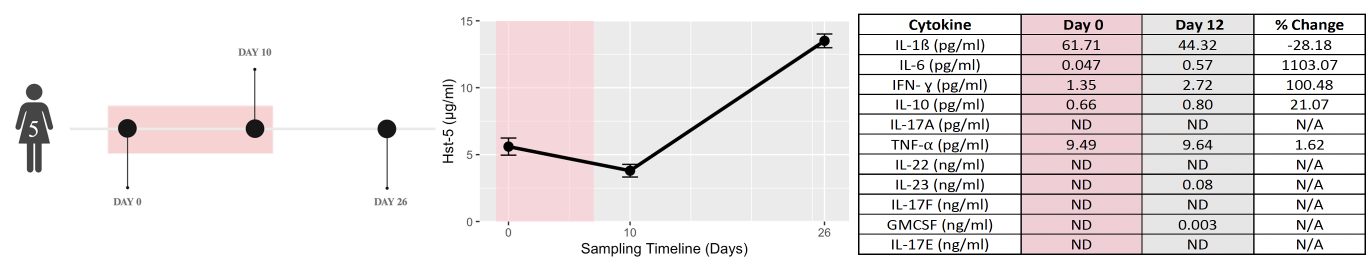
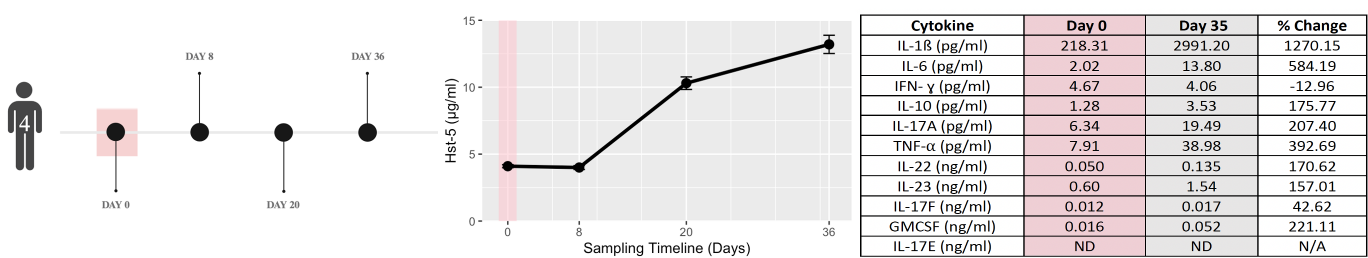
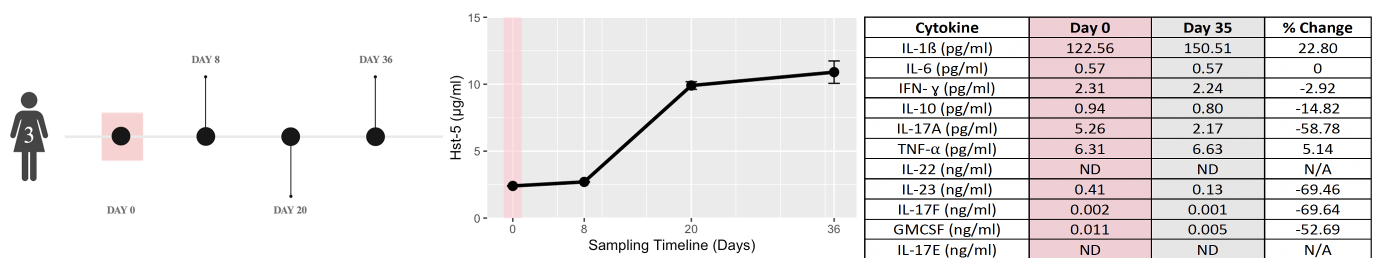
**c**



**d**



■ Pre-COVID-19 infection ■ Acute phase (COVID-19 test positive) ■ C. albicans positive ■ C. albicans negative



■ Acute phase (COVID-19 test positive)

